Volume 385, issue 1 1 November 2007 ISSN 0378-4371

PHYSICA A

STATISTICAL MECHANICS AND ITS APPLICATIONS

Recognized by the European Physical Society

Available online at
ScienceDirect
www.sciencedirect.com

http://www.elsevier.com/locate/physa

Available online at www.sciencedirect.com
ScienceDirect
Physica A 385 (2007) 221–232
PHYSICA A
www.elsevier.com/locate/physa

Adsorption in one-dimensional channels arranged in a triangular structure: Theory and Monte Carlo simulations

M. Dávila, P.M. Pasinetti, F. Nieto, A.J. Ramirez-Pastor*

Departamento de Física, Universidad Nacional de San Luis, CONICET, Chacabuco 917, D5700BWS San Luis, Argentina

Received 20 April 2007; received in revised form 1 June 2007
Available online 11 June 2007

Abstract

Adsorption thermodynamics of interacting particles adsorbed on one-dimensional channels arranged in a triangular cross-sectional structure is studied through Bragg–Williams approximation (BWA), Monte Carlo (MC) simulations and the recently reported Effective Substates approximation (ESA) [J.L. Riccardo, G. Zgrablich, W. A. Steele, Appl. Surf. Sci. 196 (2002) 138]. Two kinds of lateral interaction energies have been considered: (1) w_L, interaction energy between nearest-neighbor particles adsorbed along a single channel and (2) w_T, interaction energy between particles adsorbed across nearest-neighbor channels. We focus on the case of repulsive transversal interactions ($w_T > 0$), for which a rich variety of ordered phases are observed in the adlayer, depending on the value of the parameters $k_B T/w_T$ (being k_B the Boltzmann constant) and w_L/w_T. Comparisons between analytical data and MC simulations are performed in order to test the validity of the theoretical models. Appreciable differences can be seen for the different approximations, ESA being the most accurate for all cases.

Keywords: Adsorption isotherms; Lattice-gas models; Monte Carlo simulations; Equilibrium thermodynamics and statistical mechanics

1. Introduction

The study of interacting particles adsorbed on one-dimensional (1D) channels arranged in a triangular cross-sectional structure has been tackled in three previous contributions referred to as I, II and III, respectively, throughout this article [1–3]. The model discussed there mimics a nanoporous environment, where each 1D chain could represent a line of molecules adsorbed within interstitial channels formed between the tubes [4–6], inside nanotubes [4,7,8] or along the grooves sites formed between two adjacent tubes on the bundle surfaces [9–11]. For theoretical purposes, adsorption in these lines can be treated in the 1D lattice-gas approach [12,13]. This is, of course, an approximation to the state of real adsorbates in nanotubes, which is justified because thermodynamics and transport coefficient can be analytically resolved in these conditions.

*Corresponding author. Tel.: +54 2652 436151; fax: +54 2652 430224.
E-mail addresses: maradav@unsl.edu.ar (M. Dávila), mpasi@unsl.edu.ar (P.M. Pasinetti), fnieto@unsl.edu.ar (F. Nieto), antorami@unsl.edu.ar (A.J. Ramirez-Pastor).

0378-4371/$ - see front matter © 2007 Elsevier B.V. All rights reserved.
doi:10.1016/j.physa.2007.06.003

In I, the main thermodynamic properties of adsorption (adsorption isotherms and differential heat of adsorption) were studied through a lattice-gas model and Monte Carlo (MC) simulations. The adsorbent was modelled as 1D channels of equivalent adsorption sites arranged in a triangular cross-sectional structure. Two kinds of lateral interaction energies were considered: (1) w_L, interaction energy between nearest-neighbor particles adsorbed along a single channel and (2) w_T, interaction energy between particles adsorbed across nearest-neighbor channels. A rich variety of ordered phases were observed for repulsive transversal interactions ($w_T > 0$). The influence of each ordered structure on adsorption isotherms and differential heat of adsorption were analyzed and discussed in the context of the lattice-gas theory. In II, the calculations were extended to the configurational entropy of an adlayer. The problem was monitored by MC simulations and thermodynamic integration method in the canonical ensemble. In addition, an approximate estimation of the critical temperatures, corresponding to the critical concentrations $\theta = 1/3$, $1/2$, $2/3$, was obtained from the curves of configurational entropy as a function of the temperature.

III was a step further, analyzing the critical behavior of the adlayer by means of MC simulations and finite-size scaling techniques. Different behaviors were obtained, depending on the value of the parameters $k_B T/w_T$ (being k_B the Boltzmann constant) and w_L/w_T. Namely:

(1) For $w_L/w_T = 0$, successive planes are uncorrelated, the system is equivalent to the triangular lattice and the well-known $(\sqrt{3} \times \sqrt{3})$ [$(\sqrt{3} \times \sqrt{3})^*$] ordered phase is found at low temperatures and a coverage, θ, of $1/3$ [$2/3$].
(2) For $w_L/w_T < 0$, the formation of pairs of nearest-neighbor adsorbed particles along the lines is favored. Consequently, the $(\sqrt{3} \times \sqrt{3})$ and $(\sqrt{3} \times \sqrt{3})^*$ phases are reinforced and extend along the channels. The critical temperature decreases from 0.7817(1) for $w_L/w_T = -1$ to 0.3354(1) for $w_L/w_T = 0$.
(3) For $w_L/w_T > 0$, the $(\sqrt{3} \times \sqrt{3})$ and $(\sqrt{3} \times \sqrt{3})^*$ structures are formed in the planes at low-temperature and order along the channels in an array of alternating particles. The critical temperature increases from 0.3354(1) for $w_L/w_T = 0$ to 0.6098(5) for $w_L/w_T = 1$.

The MC technique was combined with the recently reported Free Energy Minimization Criterion Approach (FEMCA) [14], to predict the critical temperatures of the order–disorder transformation. The excellent qualitative agreement between simulated data and FEMCA results allows us to interpret the physical meaning of the mechanisms underlying the observed transitions.

In this article, we consider the same lattice-gas model as that treated in I, II and II. Here the difference is that we evaluate the adsorption properties by using two theoretical approaches. The first is the well-known Bragg–Williams approximation (BWA) for interacting particles [15] and the second is the recently reported Effective Substates approximation (ESA) [16]. The plan of the rest of paper is as follows. In Section 2 the lattice-gas model is presented. The theoretical approximations (BWA and ESA) are derived in Section 3. Simulation results and theoretical predictions are discussed and compared in Section 4. Finally, Section 5 is devoted to the conclusions.

2. The model

Numerous experimental and theoretical studies of gas adsorption on carbon nanotube bundles predict the existence of close parallel channels of adatoms when the adsorption takes place (1) in the interior of a nanotube, (2) in interstitial channels or (3) in the grooves sites on bundle surfaces. In this context, we present a simplified lattice-gas model, where each channel or unit cell has been represented by a 1D line of L adsorptive sites, with periodical boundary conditions. In order to include transverse interactions between parallel neighbor lines, these chains were arranged in a triangular structure of size $R \times R$ and periodical boundary conditions. Under these conditions all lattice sites are equivalent hence border effects will not enter our derivation. The energies involved in the adsorption process are three:

(1) ε_0, interaction energy between a particle and a lattice site.
(2) w_L, interaction energy between adjacent occupied axial sites.
(3) w_T, interaction energy between particles adsorbed on nearest-neighbor transverse sites.

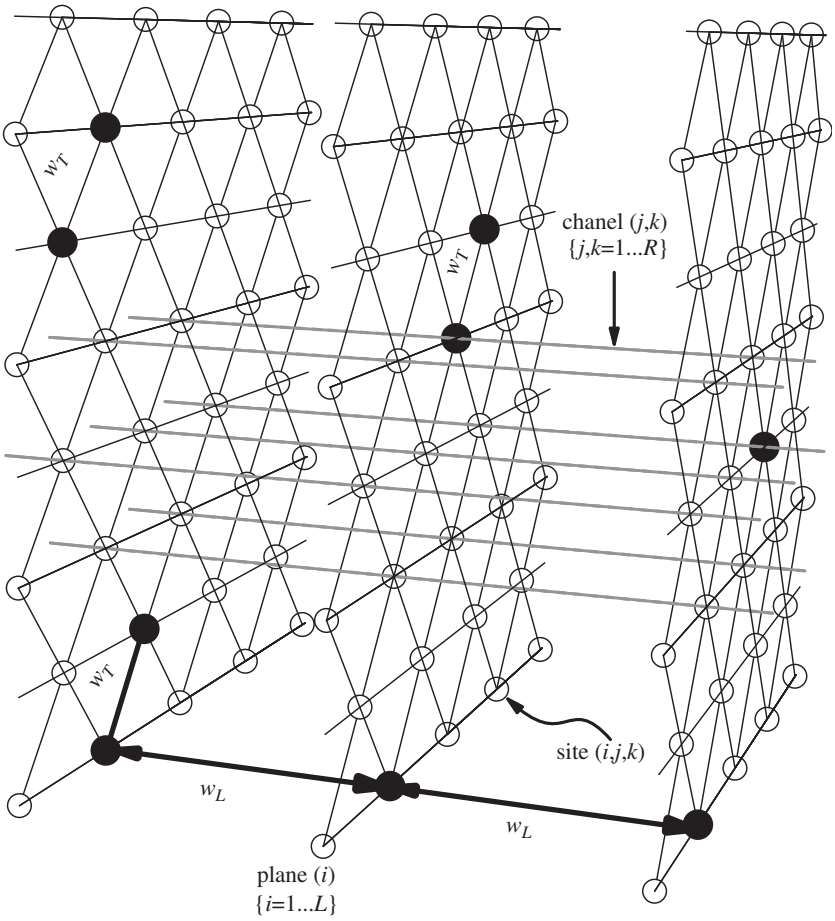

Fig. 1. Schematic representation of the studied system. Solid and open circles correspond to occupied and empty sites, respectively.

Thus, the resulting substrate is an anisotropic 3D array of $M = L \times R \times R$ adsorption sites, where each site is surrounded by two "axial" sites along the chain's axis and six "transverse" sites belonging to nearest-neighbor unit cells (see Fig. 1).

In order to describe the system of N molecules adsorbed on M sites at a given temperature T, let us introduce the local occupation variable $c_{i,j,k}$ which can take the following values: $c_{i,j,k} = 0$ if the corresponding site (i,j,k) is empty and $c_{i,j,k} = 1$ if the site is occupied by an adatom. Then, the Hamiltonian of the system is given by

$$H = w_L \sum_{\langle i,j,k;i',j',k'\rangle_L} c_{i,j,k}c_{i',j',k'} + w_T \sum_{\langle i,j,k;i',j',k'\rangle_T} c_{i,j,k}c_{i',j',k'} + (\varepsilon_0 - \mu)\sum_{i,j,k}^{M} c_{i,j,k}, \tag{1}$$

where $\langle i,j,k;i',j',k'\rangle_L$ ($\langle i,j,k;i',j',k'\rangle_T$) represents pairs of NN axial (transverse) sites and μ is the chemical potential.

The adsorption process is simulated by following the MC simulation scheme presented in I.

3. Theoretical approaches: BWA and ESA

3.1. Bragg–Williams approximation

The BWA is the most simple mean-field treatment for interacting adsorbed particles. In this context, the calculation of the canonical partition function $Q(M,N,T)$ for a system of N particles adsorbed on a lattice of

M sites (and connectivity c) at a temperature T, considering nearest-neighbor lateral interactions of magnitude w between adsorbed molecules, can be written as [15]

$$Q(M,N,T)=\frac{M!}{N!(M-N)!}\,e^{-\beta N\varepsilon}\,e^{-\beta N_{11}w}, \tag{2}$$

where $e^{-\beta N_{11}w}$ is the mean-field interaction term; N_{11} is the mean number of pairs of filled sites, each one contributing with an energy w. In general, N_{11} is calculated as follows: a molecule at a site has, on average (random distribution), $c\theta=cN/M$ occupied nearest-neighbor sites next to it; therefore, $N_{11}=(cN/M)(N/2)=cN^2/2M$, where the factor of 2 is inserted to avoid counting each 11 pair twice. In our particular case, $e^{-\beta N_{11}w}$ is changed by $e^{-\beta(N_{11}^L w_L+N_{11}^T w_T)}$, where N_{11}^L and N_{11}^T represent the mean number of pairs of filled sites along a single channel and across nearest-neighbor channels, respectively, and

$$N_{11}^L=\frac{N^2}{M}\quad\text{and}\quad N_{11}^T=\frac{6N^2}{2M}. \tag{3}$$

In the canonical ensemble, the Helmholtz free energy $F(M,N,T)$ is given by

$$F(M,N,T)=-\beta^{-1}\ln Q(M,N,T). \tag{4}$$

Thus, from Eqs. (4) and (2)

$$\beta F(M,N,T)=-\ln M!+\ln N!+\ln(M-N)!+\beta N\varepsilon+\beta\left(\frac{N^2}{M}w_L+\frac{3N^2}{M}w_T\right), \tag{5}$$

we obtain the expression for the Helmholtz free energy per site as a function of coverage $\theta=N/M$,

$$\beta f(\theta,T)=\theta\ln\theta+(1-\theta)\ln(1-\theta)+\beta\theta\varepsilon+\beta\theta^2(w_L+3w_T). \tag{6}$$

Finally, the isotherm is obtained as [15]

$$\begin{aligned}\beta\mu&=\left(\frac{\partial\beta f}{\partial\theta}\right)_T\\&=\ln\theta-\ln(1-\theta)+\beta(\varepsilon+2w_L\theta+6w_T\theta).\end{aligned} \tag{7}$$

3.2. Effective Substates approximation

The ESA has been proposed recently as an improvement over existing mean-field approximations to deal with the adsorption of interacting particles on homogeneous and heterogeneous surfaces [16].

We look at the effective adsorptive energy ε on a given site of a surface with an energy distribution $f(\varepsilon)$, as an energy level of an adsorbed particle. Due to lateral interactions, this energy level is effectively split into a number of sublevels, or substates:

$$\varepsilon_\gamma=\varepsilon+w_\gamma, \tag{8}$$

where w_γ is the interaction energy of the particle adsorbed on a given site with a neighborhood characterized by index γ (for example, $1NN$ and $2NNN$ occupied sites, etc.). Then, assuming that (*i*) each site can only be occupied by a single particle, and (*ii*) the effective energy levels ε_γ are different (this is strictly true for a continuous distribution of adsorptive energies), the statistical ensemble of N adsorbed particles would be described by the Fermi-Dirac statistics:

$$A_\gamma(\varepsilon)=\frac{\exp\left[-((\varepsilon+w_\gamma-\mu)/k_BT)\right]}{1+\exp\left[-((\varepsilon+w_\gamma-\mu)/k_BT)\right]}, \tag{9}$$

where $A_\gamma(\varepsilon)$ is the mean occupancy number of the substate ε_γ.

The mean occupancy of a given site, θ_L (the local coverage), is then given by

$$\theta_L=\sum_\gamma P_\gamma A_\gamma(\varepsilon), \tag{10}$$

where P_γ is the probability of occurrence of the sublevel γ (in other words, the local configuration characterized by the index γ).

The overall mean coverage θ, i.e. the overall adsorption isotherm, can finally be expressed as

$$\theta(\mu, T) = \int f(\varepsilon)\theta_L(\varepsilon)\,\mathrm{d}\varepsilon. \tag{11}$$

P_γ can be obtained through a mean-field approximation, by assuming that all sites are occupied with the same probability θ. Then, for example, if γ stands for any configuration where γ sites are occupied out of a total of c NN sites, then we would have:

$$P_\gamma = \binom{c}{\gamma}\theta^\gamma(1-\theta)^{c-\gamma}. \tag{12}$$

By replacing Eq. (12) in Eqs. (10) and (11), we would get a polynomial in θ whose solution gives the global adsorption isotherm.

In order to apply this approximation to our system, we consider a homogeneous surface and distinguish two kinds of nearest-neighbor sites: (*i*) nearest-neighbor along a single channel (“axial” sites) and (*ii*) sites across nearest-neighbor channels (“transverse” sites).

We now introduce the probability P_{γ_L,γ_T} of finding an occupied site, with γ_L and γ_T nearest-neighbor occupied sites along a single channel and across nearest-neighbor channels, respectively. These probabilities can be obtained as

$$P_{\gamma_L,\gamma_T} = \binom{2}{\gamma_L}\theta_1^{\gamma_L}(1-\theta_1)^{2-\gamma_L}\binom{6}{\gamma_T}\theta_1^{\gamma_T}(1-\theta_1)^{6-\gamma_T}\{\gamma_L = 0,\ldots,2;\gamma_T = 0,\ldots,6\}. \tag{13}$$

In addition, the mean occupancy number of a substate having an occupied site with γ_L and γ_T nearest-neighbor occupied sites, A_{γ_L,γ_T}, is

$$A_{\gamma_L,\gamma_T} = \frac{\exp[-((\varepsilon_K + \gamma_L w_L + \gamma_T w_T - \mu)/k_BT)]}{1+\exp[-((\varepsilon_K + \gamma_L w_L + \gamma_T w_T - \mu)/k_BT)]} \quad \{\gamma_L = 0,\ldots,2;\gamma_T = 0,\ldots,6\}. \tag{14}$$

Finally, the overall mean coverage θ is obtained from the integral in Eq. (11), which reduces to the sum,

$$\theta = \sum_{\gamma_L=0}^{2}\sum_{\gamma_T=0}^{6} P_{\gamma_L,\gamma_T}A_{\gamma_L,\gamma_T}. \tag{15}$$

The last equation is easily calculated through a standard computing procedure (in our case, we used Maple software).

4. Results and discussion

We focus on the case of repulsive transverse interactions among adsorbed particles ($w_T > 0$) since, as we shall see, interesting structures appear in the adsorbed phase. In addition, repulsive and attractive longitudinal lateral interactions were considered.

The computational simulations have been performed for $L = 96$ in the direction along the axis of the nanotubes and $R = 60$ in the transversal direction. With this size of the lattice, we verified that finite-size effects are negligible. In order to rationalize our analysis, five different cases have been considered, according to the lateral interaction energies involved in the adsorption process:

Case I: $w_L/w_T = 0$ ($w_L = 0$) and $w_T/k_BT > 0$.
Case II: $w_T/k_BT = 10$ ($w_T = 1$ and $k_BT = 0.1$) and $w_L/w_T > 0$.
Case III: $w_T/k_BT = 10$ ($w_T = 1$ and $k_BT = 0.1$) and $w_L/w_T < 0$.
Case IV: $w_L/k_BT = 10$ ($w_L = 1$ and $k_BT = 0.1 =$) and $w_T/w_L > 0$.
Case V: $w_L/k_BT = -10$ ($w_L = 1$ and $k_BT = 0.1 =$) and $w_T/w_L < 0$.

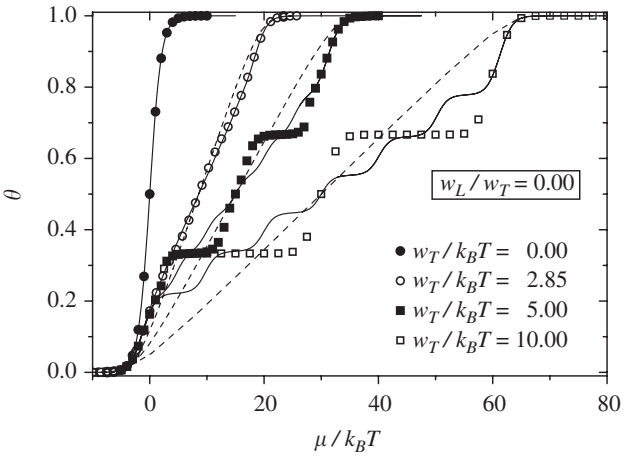

Fig. 2. Adsorption isotherms for $w_L/w_T = 0$ and different values of w_T/k_BT as indicated. Symbols, dashed lines and solid lines represent MC, BWA and ESA calculations, respectively.

In order to understand the basic phenomenology, in Fig. 2 we consider adsorption isotherms for *Case I*, being $w_T/k_BT(= 0; 1.5; 3; 5$ and $10)$. In this situation, successive planes are uncorrelated and the system is equivalent to the well-known triangular lattice in two dimensions. In the limit $w_T/k_BT \to 0$, the coverage grows monotonically with the chemical potential and the corresponding isotherm is Langmuir type. For higher values of w_T/k_BT (see for example $w_T/k_BT = 10$), three regimes appear in the isotherms. First, the admolecules occupy the lattice up to a $(\sqrt{3} \times \sqrt{3})$ ordered phase is formed at $\theta = 1/3$. This corresponds to the first "plateau" in Fig. 2. The second plateau appears at $\theta = 2/3$ and corresponds to the presence of a $(\sqrt{3} \times \sqrt{3})^*$ structure on the substrate. Finally, the filling of the lattice is completed. The plateaus in the isotherm (structural rearrangements in the adlayer) are clearly associated to the existence of a order–disorder phase transition in the adsorbate.

BWA (dashed lines) agrees with simulation data only for $T \to \infty$. As the temperature decreases, the difference between BWA and MC simulation gets more important. On the other hand, ESA (solid lines) is a good approach to low and high coverage even at low temperature. At intermediate coverage, the ESA predicted isotherms are clearly very rough for nearly homogeneous surfaces in the coverage region where the order–disorder phase transition has a strong effect. This is obviously due to the independent site approximation done in calculating the probability P_{γ_L,γ_T} of the sublevel (γ_L, γ_T) (Eq. (13)).

Case II is studied in Fig. 3. As it can be observed, a new plateau appears in the adsorption isotherm at $\theta = 1/2$ as w_L/w_T is increased. This behavior indicates the presence of an ordered structure at half coverage. In fact, planes are filled up to $\theta = 1/2$ with mean energy per site equal to $w_T/2$ (each adsorbed particle is surrounded by two occupied nearest-neighbors in the plane). Then, successive planes are occupied avoiding the formation of monomer–monomer pairs along the nanotubes. At $\theta = 1/3$, the $(\sqrt{3} \times \sqrt{3})$ ordered structure is formed in the planes for all values of w_L/w_T with mean energy per site equal to 0. Then, adatoms avoiding configurations with nearest-neighbor interactions order along the channels in a structure of alternating particles. The behavior of the system at $\theta = 2/3$ can be understood from the equivalence vacancy-particle. A typical case ($w_T/k_BT = 10$ and $w_L/w_T = 0.50$) obtained by MC simulations in the grand canonical ensemble (symbols) and comparison with BWA (dashed lines) and ESA (solid lines) is shown in the inset of Fig. 3. BWA and ESA do not predict the existence of ordered phases in the adsorbate, and it is not possible to distinguish the different adsorption regimes. Note that even in these circumstances, ESA is a good approach to low and high coverage.

Fig. 4 shows the results obtained for *Case III*. Attractive monomer–monomer longitudinal interactions favor the formation of pairs of nearest-neighbor adsorbed particles along the nanotubes. Consequently, the $(\sqrt{3} \times \sqrt{3})$ and $(\sqrt{3} \times \sqrt{3})^*$ ordered phases "propagate" along the channels and the plateaus (steps) in the adsorption isotherm (differential heat of adsorption) are reinforced. As expected for attractive w_L interactions, isotherms shift to lower values of μ/k_BT and their slopes raise as the ratio w_L/k_BT increases. In the case of

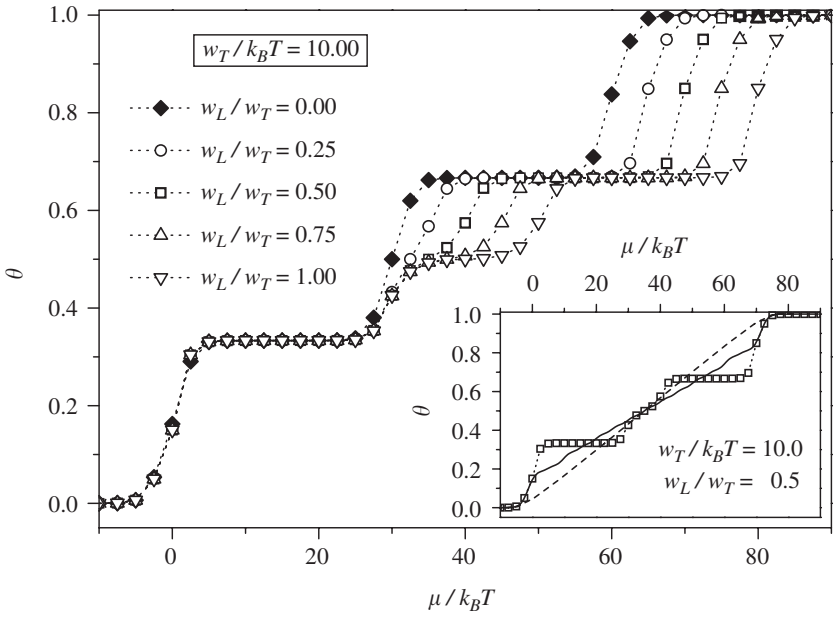

Fig. 3. Adsorption isotherms for $w_T/k_BT = 10$ ($w_T = 1$ and $k_BT = 0.1$) and different values of $w_L/w_T > 0$ as indicated. Inset: Comparison between MC (symbols), BWA (dashed line) and ESA (solid line) calculations for $w_T/k_BT = 10$ and $w_L/w_T = 0.5$.

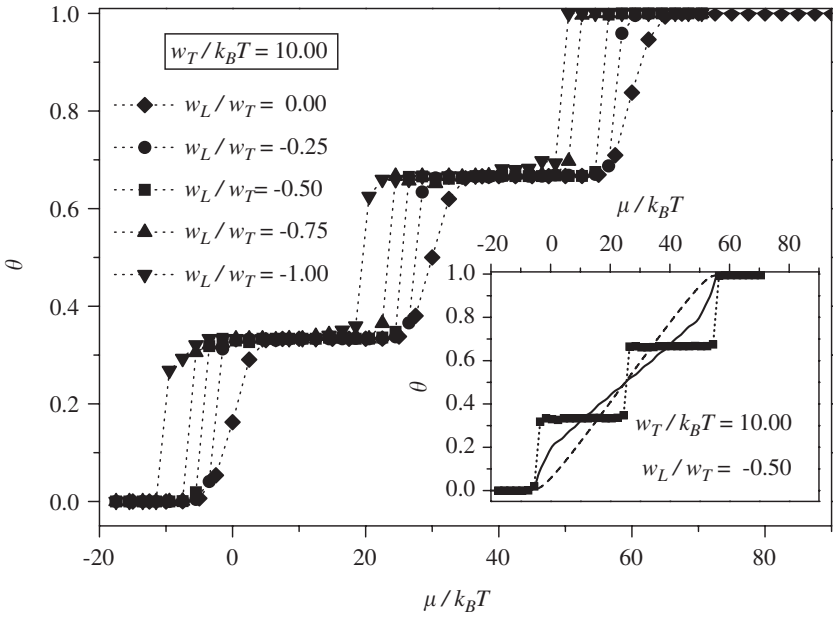

Fig. 4. Adsorption isotherms for $w_T/k_BT = 10$ ($w_T = 1$ and $k_BT = 0.1$) and different values of $w_L/w_T < 0$ as indicated. Inset: Comparison between MC (symbols), BWA (dashed line) and ESA (solid line) calculations for $w_T/k_BT = 10$ and $w_L/w_T = -0.5$.

BWA and ESA (see inset), the disagreement turns out to be large for intermediate θ values, and a good approximation is recovered for low and high coverage.

To complete our simulation analysis, we study the effect of varying the transversal lateral interaction as the longitudinal interaction is fixed. For this purpose, the adsorption isotherms for *Cases IV* and *V* are shown in Figs. 5 and 6, respectively. The curves for $w_L/k_BT = 10$, $w_T/w_L = 1$ (open down triangles in Fig. 5) and $w_L/k_BT = -10$, $w_T/w_L = -1$ (solid down triangles in Fig. 6), are taken as starting point and, then, the transversal repulsive interaction is diminished while w_L/k_BT remains constant. In these cases, the adlayer changes from a 3D fluid for $|w_T/w_L| > 0$ to a 1D fluid for $w_T/w_L = 0$. For attractive (repulsive) longitudinal

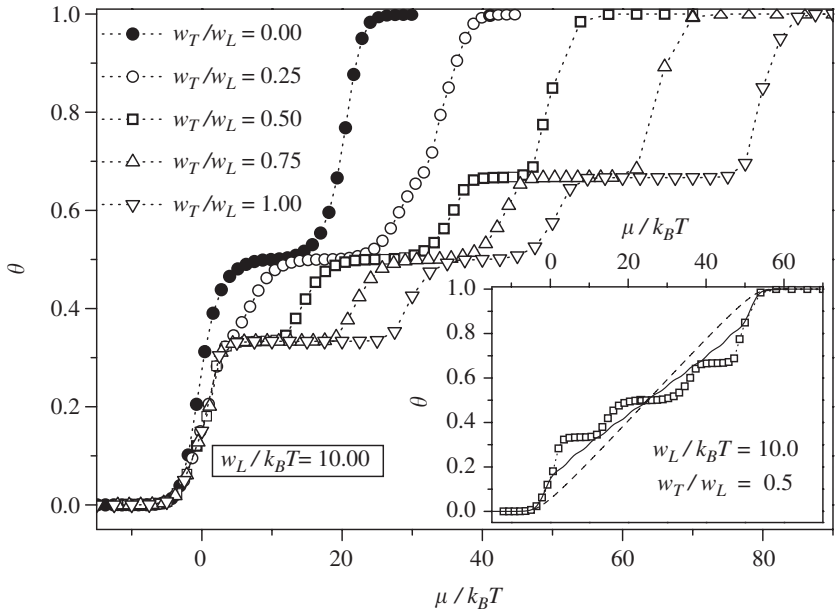

Fig. 5. Adsorption isotherms for $w_L/k_BT = 10$ ($w_L = 1$ and $k_BT = 0.1$) and different values of $w_T/w_L > 0$ as indicated. Inset: Comparison between MC (symbols), BWA (dashed line) and ESA (solid line) calculations for $w_L/k_BT = 10$ and $w_T/w_L = 0.5$.

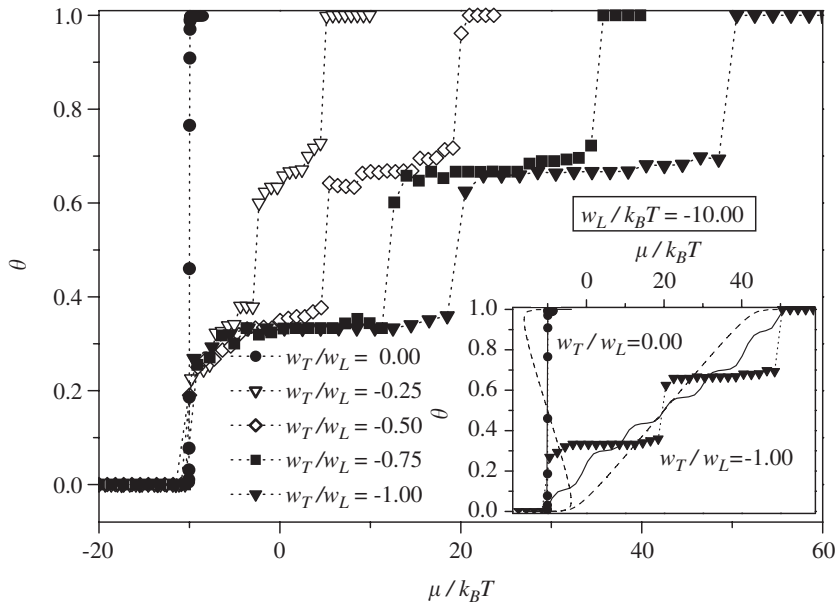

Fig. 6. Adsorption isotherms for $w_L/k_BT = -10$ ($w_L = -1$ and $k_BT = 0.1$) and different values of $w_T/w_L < 0$ as indicated. Inset: Comparison between MC (symbols), BWA (dashed line) and ESA (solid line) calculations for $w_L/k_BT = -10$ and two values of w_T/w_L [$w_T/w_L = 0$ (circles) and $w_T/w_L = -1.0$ (triangles)].

energies and null transversal interactions, the isotherm develops a marked jump between low and high coverage (a neat step at $\theta = 1/2$). It is worth noticing that although the jump (plateau) in the isotherm may be indicative of a first-order (second-order) phase transition, the system does not show a phase transition at finite temperature. It is well known that no phase transition develops in a 1D lattice when weak coupling between neighboring particles exists.

With respect to the comparison with BWA and ESA, an interesting behavior is shown in the inset of Fig. 6 for the case $w_L/k_BT = -10$ and $w_T/w_L = 0$. In fact, while BWA shows the typical van der Waals loop characteristic of the first-order phase transitions, MC and ESA agree extremely good. This finding confirms

previous results in the literature [16], where ESA showed an excellent behavior for attractive particles on 1D lattices. As an example, the exact $T_c = 0$ (1D) is obtained from ESA in Ref. [16].

In all cases (Figs. 2–6), ESA is a good approach which behaves better than BWA. The quantitative differences between simulation and theoretical results can be much easily rationalized with the help of the absolute error, $\varepsilon^a(\theta)$, which is defined as

$$\varepsilon^a = |\mu_{theor} - \mu_{sim}|_\theta, \tag{16}$$

where μ_{sim} (μ_{theor}) represents the chemical potential obtained by using MC simulation (analytical approach). Each pair of values (μ_{sim}, μ_{theor}) is obtained at fixed θ.

As an example, in Fig. 7 we show $\varepsilon^a(\theta)$ for a typical case (*Case II*). The curves corresponding to BWA and ESA are shown in parts (a) and (b), respectively. The differences between BWA and ESA are very appreciable [see part (c)].

In order to compare all studied cases, we define the integral error ε^i, which takes into account the differences between theoretical and simulation data in all range of coverage,

$$\varepsilon^i = \int_0^1 \varepsilon^a(\theta)\,\mathrm{d}\theta. \tag{17}$$

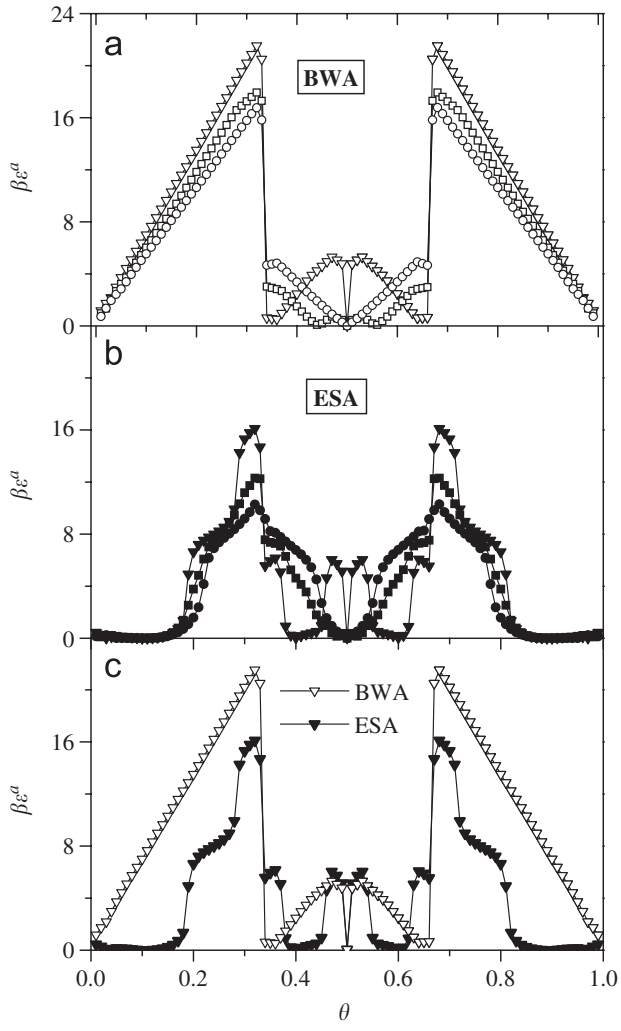

Fig. 7. Absolute error in k_BT units, $\beta\varepsilon^a$, versus surface coverage for adsorption isotherms corresponding to Case II ($w_T/k_BT = 10$ and $w_L/w_T > 0$). The symbology is as follows: circles, $w_L/w_T = 0.25$; squares, $w_L/w_T = 0.50$ and triangles, $w_L/w_T = 1.0$. (a) BWA results. (b) ESA results. (c) Comparison between BWA and ESA for a typical case at low temperature ($w_T/k_BT = 10$ and $w_L/w_T = 1.0$).

The integral error is shown in Fig. 8 for all studied cases. We corroborate that always ESA is a better approximation than BWA for all values of w_L/w_T.

From the theoretical point of view, future efforts will be directed to include the nearest-neighbor interactions by following the configuration-counting procedure of the well-known Quasi-Chemical approach (QCA) [15]. For this purpose, the probabilities P_γ's will be recalculated in the new theoretical framework. This refinement, which in essence means that pairs of nearest-neighbor sites are treated as independent of each other, will represent a qualitative advance with respect to the BWA, which is equivalent to giving all configurations of N molecules on M sites the same weight as they would have $w = 0$ (correlations between pair of particles are neglected).

As it can be observed from Figs. 2–6, the presence of repulsive lateral interactions results in the existence of pronounced plateaus in the adsorption isotherms. These features, which are clear evidences of the formation of ordered structures in the adlayer, are not well reproduced by mean-field approximations, where the main thermodynamic functions present a monotonous behavior. In this context, the introduction of local correlations via QCA seems to be a promising way toward a more accurate description of the singularities appearing in the adsorption isotherms as the temperature lowers.

Finally, it is of interest to discuss the applicability of the present model to interpret experimental data. It is clear that a complete analysis of the phenomenon of adsorption of gases in quasi-1D is a quite difficult subject

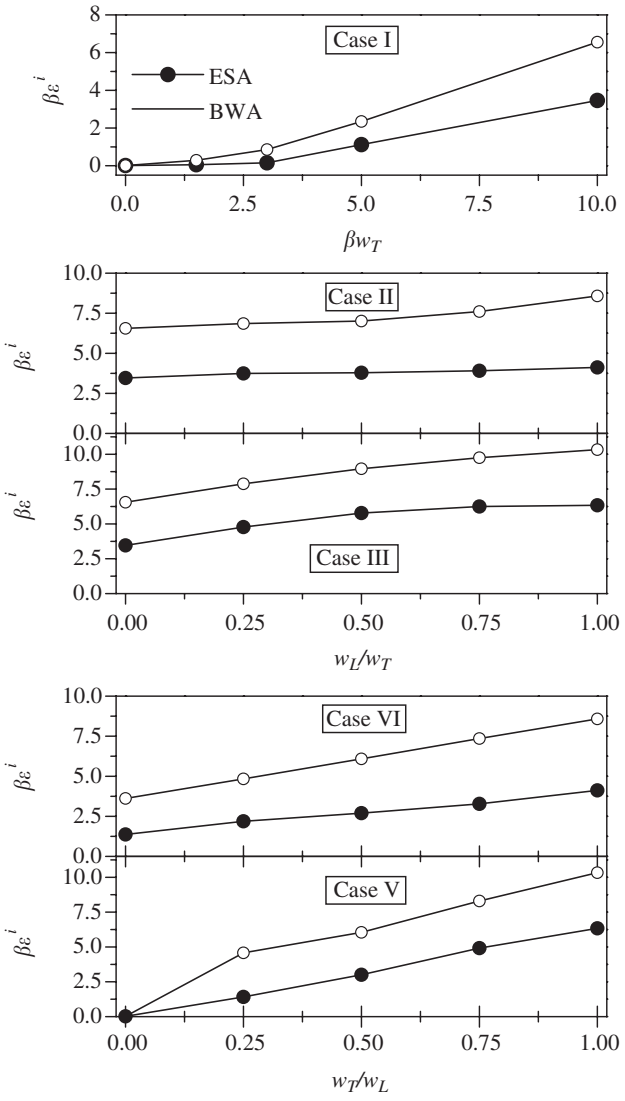

Fig. 8. Integral error in k_BT units, $\beta\varepsilon^i$, versus lateral interaction for Cases I–V as indicated.

because of the complexity of the involved systems. For this reason, the understanding of simple models with increasing complexity might be a help and a guide to establish a general framework for the study of this kind of systems. In this sense, several conclusions can be drawn from the present work:

- Depending on the values of the parameters of the system, the adlayer behaves as a 1D, 2D or 3D fluid. Thus, for $w_T/w_L = 0$ ($w_L \neq 0$), the chains do not interact with each other and the system is equivalent to a 1D lattice-gas; for $w_L/w_T = 0$ ($w_T \neq 0$), successive transversal planes are uncorrelated and the system is equivalent to the well-known triangular lattice in 2D; and for $w_L/w_T = 0 \neq 0$, the adlayer behaves as a 3D fluid. Similar dimensional crossover has been observed and discussed in Refs. [4,5,10].
- When the attractive interactions are significant (see *Case V*), the typical van der Waals loops are observed in the theoretical adsorption isotherms. This type of behavior has been already discussed in Refs. [7,8] and could be useful to interpret data from experiments involving first-order phase transitions (condensation transitions).
- Interesting orientational effects, such as the recently reported in Ref. [9] for CO_2 adsorbed in the groove sites of carbon nanotubes, could be treated in the framework of the present model, after the inclusion of multisite-occupancy adsorption. This task, which means to consider admolecules occupying more than one site, is in progress.

5. Conclusions

In the present work, the adsorption of monomers on low-dimensional systems was analyzed. In particular, a simple lattice-gas model of a nanoporous environment was studied, where each nanotube or unit cell was represented by a one-dimensional array. These chains were arranged in a triangular cross-sectional structure. Such study was carried out through of Monte Carlo simulation and two analytical approaches: Bragg–Williams and Effective Substates approximations (BWA and ESA).

Depending on the relationship between longitudinal and transversal interactions, different behaviors were observed in the adsorption isotherms. Though the analytical approaches do not reproduce the simulation results for high values of the lateral interactions, there exists a wide range of $w_L(T)/k_BT$, where ESA provides an excellent fitting of the simulation data. In addition, most of the experiments in surface science are carried out in this range of interaction energy. Then, ESA not only represents a qualitative advance with respect to the BWA, but also gives a framework and compact equations to consistently interpret thermodynamic adsorption experiments.

Acknowledgments

This work was supported in part by CONICET (Argentina) under project PIP 6294; Universidad Nacional de San Luis (Argentina) under projects 328501 and 322000 and the National Agency of Scientific and Technological Promotion (Argentina) under project 33328 PICT 2005. The numerical work were done using the BACO parallel cluster (composed by 60 PCs each with a 3.0 MHz Pentium-4 processors) located at Laboratorio de Ciencias de Superficies y Medios Porosos, Universidad Nacional de San Luis, San Luis, Argentina.

References

[1] P.M. Pasinetti, J.L. Riccardo, A.J. Ramirez-Pastor, Physica A 355 (2005) 383.
[2] P.M. Pasinetti, J.L. Riccardo, A.J. Ramirez-Pastor, J. Chem. Phys. 122 (2005) 154708.
[3] P.M. Pasinetti, F. Romá, J.L. Riccardo, A.J. Ramirez-Pastor, J. Chem. Phys. 125 (2006) 214705.
[4] M.M. Calbi, S.M. Gatica, M.J. Bojan, G. Stan, M.W. Cole, Rev. Mod. Phys. 73 (2001) 857.
[5] M.M. Calbi, M.W. Cole, Phys. Rev. B 66 (2002) 115413.
[6] M.M. Calbi, J.L. Riccardo, Phys. Rev. Lett. 94 (2005) 246103.

[7] R.A. Trasca, M.M. Calbi, M.W. Cole, Phys. Rev. E 65 (2002) 061607.
[8] R.A. Trasca, M.M. Calbi, M.W. Cole, J.L. Riccardo, Phys. Rev. E 69 (2004) 011605.
[9] L. Chen, J.K. Johnson, Phys. Rev. Lett. 94 (2005) 125701.
[10] J.V. Pearce, M.A. Adams, O.E. Vilches, M.R. Johnson, H.R. Glyde, Phys. Rev. Lett. 95 (2005) 185302.
[11] L. Heroux, V. Krungleviciute, M.M. Calbi, A.D. Migone, J. Phys. Chem. B 110 (2006) 1297.
[12] A.J. Ramirez-Pastor, T.P. Eggarter, V.D. Pereyra, J.L. Riccardo, Phys. Rev. B 59 (1999) 11027.
[13] F. Romá, A.J. Ramirez-Pastor, Phys. Rev. E 69 (2004) 036124.
[14] F. Romá, A.J. Ramirez-Pastor, J.L. Riccardo, Phys. Rev. B 68 (2003) 205407.
[15] T.L. Hill, An Introduction to Statistical Thermodynamics, Addison-Wesley, Reading, MA, 1960.
[16] J.L. Riccardo, G. Zgrablich, W.A. Steele, Appl. Surf. Sci. 196 (2002) 138.